MSUCL-226
November 1976

Calculation of Recoil-Order Matrix Elements for the Beta Decays of ^{20}F and ^{20}Na*

Frank P. Calaprice†
Department of Physics
Princeton,University, Princeton, New Jersey 08540

and

W. Chung and B. H. Wildenthal
Cyclotron Laboratory, Michigan State University,
East Lansing, Michigan 48824

ABSTRACT

The matrix elements which affect the shapes of the beta spectra and the beta-gamma angular correlations are calculated for the ^{20}F - ^{20}Na mirror GT decays to the 1634 keV level of ^{20}Ne. The dominant effects are due to the weak-magnetism and the axial-vector tensor form factors. Matrix elements relevant to the beta-alpha correlations for other ^{20}Na decays are also evaluated, with similar conclusions.

*Work supported by the U. S. National Science Foundation

†Alfred P. Sloan Fellow

I. Introduction

Some of the best tests for the presence of the second-class[1] weak interaction involve measurements of certain angular correlations[2] in nuclear beta decay. The βγ correlations for the mirror Gamow-Teller decays of the mass-20 system are particularly interesting in this respect, because of the relative simplicity of the decay schemes and the large energies released.

To first order in recoil, the βγ correlation depends on a linear combination of the weak magnetism and the axial-vector tensor form factors. For $\Delta T = 1$ decays the form factors are each, in principle, combinations of first and second class components. Thus to determine the second class tensor term it is usually necessary to invoke the CVC theory to determine the weak magnetism form factor and to combine the βγ correlations of mirror e^+ and e^- decays to eliminate the first class tensor form factor. To higher order in recoil, other form factors also contribute and the procedure of isolating second-class contributions becomes a little more complicated. In order to assess the importance of these higher order form factors in the case of the A=20 decays, we have evaluated them with nuclear shell model wave functions.

Our procedure is to utilize the relationships between the nuclear form factors and matrix elements of one-body operators, which are given by the impulse approximation.[2] While the validity of the impulse approximation can be questioned for these higher order terms, there is evidence that the extended shell model is adequate for calculating the matrix elements. Within the limitations of this procedure we evaluate the form factors and their effect on the beta-gamma correlations. In addition, we calculate the shapes of the beta spectra with the goal of assessing the possibility of determining the weak magnetism form factor from the spectrum shape. Finally, we have attempted to present these results for A=20 in a thoroughly detailed context so that comparable analyses in other sd shell nuclei

can be carried out in a straightforward fashion from other nuclear wave functions.

II. Discussion of Decay Process

A simiplified version of the mass-20 decay scheme is illustrated in Fig. 1. The decay rate for unpolarized nuclei for a process in which the beta particle is detected in coincidence with the delayed E2 gamma ray (spins and neutrino unobserved) is given by the following[2]

$$d\lambda = \frac{G_v^2 \cos^2\theta_c}{2(2\pi)^5} F_o(Z,E)\, pE\, (E_o-E)^2\, dE\, d\Omega_e\, d\Omega_\gamma \tag{1}$$

$$\times \left\{ G_o(E) + \Delta_1(E)\frac{p}{E}\cos\theta + \frac{1}{2}G_2(E)\left(\frac{p}{E}\right)^2(\cos^2\theta - \tfrac{1}{3}) \right\}$$

In the above, p and E are the beta momentum and total energy, respectively G_v and θ_c are the vector coupling constant and Cabibbo angle, F_o is the point charge Fermi function and θ is the angle between the beta and gamma particle directions. The spectral functions $G_o(E)$, $\Delta_1(E)$ and $G_2(E)$ for Gamow-Teller decays are given by the following:

$$G_o(E) = c_1^2 - \frac{2}{3}\frac{E_o}{M}c_1(c_1 + d^I \pm b \pm d^{II}) + \frac{2}{3}\frac{E}{M}c_1(5c_1 \pm 2b)$$

$$- \frac{1}{3}\frac{m_e^2}{ME}\left[2c_1^2 + c_1(d^I \pm 2b \pm d^{II}) - \frac{E_o - E}{2M}c_1 h\right]$$

$$+ \frac{2}{9}c_1c_2(11\, m_e^2 + 20\, EE_o - 20\, E^2 - 2\, m_e^2 E_o/E) \tag{2}$$

$$\Delta_1(E) = -\frac{19}{9}\frac{E}{M}\left(1 - \frac{1}{19}\frac{E_o}{E}\right)c_1^2 . \tag{3}$$

$$G_2(E) = \frac{E}{2M}\left\{(c_1^2 \pm c_1 b \mp c_1 d^{II} - c_1 d^I) + \frac{8}{3}c_1c_2(E_o - E)M\right.$$

$$- \frac{1}{\sqrt{14}}\left(\pm\sqrt{\frac{3}{2}}\frac{E_o - E}{M}c_1 g \pm 3c_1 f + \frac{3(E_o - 2E)}{2M}c_1 j_2\right)$$

$$\left. - \frac{3}{\sqrt{35}}\frac{E}{M}c_1 j_3 \right\}. \tag{4}$$

The quantity M is the nuclear mass while c, b, d, f, g and h denote the nuclear form factors. The latter are given in Table I in terms of matrix elements, as predicted by the impulse approximation. The matrix elements are defined in Table II. The dominant form factor is the Gamow-Teller (c_1) term and the terms of next order of importance are b and d, the weak magnetism and the tensor form factors, respectively. In the above, Coulomb nuclear size effects are neglected.

It is common to express the beta-gamma correlation in the form

$$d\lambda \simeq 1 + A_{\beta\gamma}\frac{p}{E}\cos\theta + B_{\beta\gamma}\left(\frac{p}{E}\right)^2\cos^2\theta \tag{5}$$

whence the correlation coefficients are given by

$$A_{\beta\gamma} = \Delta_1(E)/(G_o(E) - \tfrac{1}{6}G_2(E)) \tag{6}$$

and

$$B_{\beta\gamma} = \tfrac{1}{2}G_2(E)/(G_o(E) - \tfrac{1}{6}G_2(E)). \tag{7}$$

The beta-alpha correlations for the ^{20}Na decays to unbound 2^+ levels of ^{20}Ne have a similar form[2]

$$d\lambda \approx 1 + A_{\beta\alpha} \frac{p}{E} \cos\theta + B_{\beta\alpha} \left(\frac{p}{E}\right)^2 \cos^2\theta, \qquad (8)$$

where the main difference is a factor of two for the $\cos^2\theta$ term. There is also a slight change in the coefficient of $\cos\theta$

$$A_{\beta\alpha} = \Delta_1'(E)/(G_o(E) - \tfrac{1}{3} G_2(E)) \qquad (9)$$

$$B_{\beta\alpha} = G_2(E)/(G_o(E) - \tfrac{1}{3} G_2(E)) \qquad (10)$$

where $\Delta_1'(E) = \frac{2E}{Mv^*} c_1^2$.

The $\cos\theta$ correlation arises from a center-of-mass to laboratory transformation. The quantity v^* is the speed of the secondary particle (gamma ray or alpha particle) with respect to the recoil ^{20}Ne system. For the $\beta\gamma$ correlations the kinematic A coefficient is very small since v^* is the speed of light but for $\beta\alpha$ correlations A is comparable to B.

The shape of the momentum spectrum for unpolarized nuclei is specified by the spectral function $G_o(E)$. Finite nuclear size and additional coulomb effects have been calculated and the more accurate expression for the spectrum is given by the following[2,3]

$$d\lambda = \frac{4}{(2\pi)^3} G_v^2 \cos^2\theta_c R(E, E_o) F(Z,E) p^2 (E_o - E)^2 h_1(E) dp \qquad (11)$$

Here $R(E,E_o)$ is a correction for bremsstrahlung, $F(Z,E)$ is the Fermi function calculated for a finite size uniformly charged nucleus, and $h_1(E)$ is the spectral function which is similar to $G_o(E)$ except for the Coulomb and finite size correction terms

$$h_1(E) = c_1^2 + \frac{2}{9} c_1 c_2 (11 m_e^2 + 20 EE_o - 2 m_e^2 E_o/E - 20 E^2)$$

$$- c_1 c_2 \left[\frac{9}{2} \left(\frac{\alpha Z}{R}\right)^2 \mp \frac{4}{3} \frac{\alpha Z E_o}{R} \pm \frac{22}{3} \frac{\alpha Z E}{R}\right]$$

$$+ \frac{\sqrt{10}}{6} \frac{\alpha Z}{MR} c_1 (2b \pm d^I + d^{II} \pm c_1)$$

$$- \frac{2}{3} \frac{E_o}{M} c_1 (c_1 + d^I \pm d^{II} \pm b) + \frac{2}{3} \frac{E}{M} c_1 (5c_1 \pm 2b)$$

$$- \frac{1}{3} \frac{m_e^2}{ME} [2c_1^2 + c_1 (d^I \pm 2b \pm d^{II}) - \frac{E_o - E}{2M} c_1 h]. \qquad (12)$$

This form for $h_1(E)$ is correct if the Behrens-Jänecke Fermi function is used.[3] The dependence of the Gamow-Teller form factor on the momentum transfer q is accounted for by the term c_2, defined by

$$c(q^2) = c_1 + q^2 c_2 . \qquad (13)$$

To determine the second class tensor form factor, d^{II}, one must combine measurements of the B correlation coefficient for both $e^\pm$ decays, so as to cancel the first class term d^I. The difference of the B coefficients for $e^\pm$ decays, with the same E_o and at the same E, depends on $(b - d^{II})$ and on the higher order vector terms g and f.

The form factors b, g and f arise from the vector interaction and can therefore be determined from the experimental decay rates for the analog gamma decay by CVC theory. In terms of the isovector radiative widths, $\Gamma^{T=1}$, the important relationships are[2]

$$\Gamma_{M1}^{T=1} = \frac{1}{6} \alpha E_\gamma^3 b^2/M^2 \qquad (14)$$

$$\Gamma_{E2}^{T=1} = \frac{1}{30} \alpha E_\gamma^5 M_Q^2 /(\hbar c)^4 \qquad (15)$$

Here $\alpha = 1/137.04$ is the fine structure constant, E_γ is the gamma ray transition energy, and M_Q is the matrix element of the quadrupole moment operator, which is related to f and g as given in Table I.

With the correlation coefficients for both decays determined by measurement and by using CVC it is thus possible to determine d^{II} in a model independent way. Unfortunately, the end-point energies for the A=20 decays differ considerably, $E_o(^{20}F)$=5.9 MeV and $E_o(^{20}Na)$=11.7 MeV, and this makes the above cancellation of the first class form factors j_2 and j_3 problematic. This point will be dealt with below.

It should be noted that the shape of the beta spectrum depends on b but is insensitive to d^{II}. This provides the opportunity to determine b, independently of d^{II}, and thus check CVC, provided the c_1c_2 terms are not too large. If the latter are large one can combine the spectra for the e^+ and e^- decays to eliminate these terms (except for the c_1c_2 αZ term). However, such a procedure also cancels a possible second class contribution to b and therefore it tests a more restricted form of CVC.[3] The strong form of CVC, of course, rules out a second class vector current. It was, in part, for this reason that our calculation of c_2/c_1 was carried out.

Before discussing the wave functions and the calculations, we settle some points concerning the definitions of operators and reduced matrix elements. First, the isospin operator $\tau^\pm$ is such that $\tau_3|P\rangle=\frac{1}{2}|P\rangle$, where $|P\rangle$ is the proton state. Second, the reduced matrix elements of Table II do not conform to conventional definitions, but are instead defined for an irreducible tensor operator O^m_k of rank k by the expression

$$\langle J_\beta M_\beta | (O^m_k)^* | J_\alpha M_\alpha \rangle = C^{M_\beta\ mM}_{J_\beta\ kJ_\alpha} \langle J_\beta || O_k || J_\alpha \rangle_{HT} , \qquad (16)$$

where the subscript HT denotes Holstein-Treiman.[4] The matrix elements of Table II are reduced in ordinary spin but not isospin. In the present calculations, however, we work with the reduced matrix elements of de Shalit and Talmi[5] (dST), which are defined by

$$\langle J_\beta M_\beta | O^m_k | J_\alpha M_\alpha \rangle = \frac{1}{\sqrt{2J_\beta + 1}} C^{M_\alpha\ mM_\beta}_{J_\alpha\ kJ_\beta} \langle J_\beta || O_k || J_\alpha \rangle_{dST} \qquad (17)$$

The relationship between the two definitions of the reduced matrix elements is

$$\langle J_\beta || O_k || J_\alpha \rangle_{HT} = \frac{(-1)^{J_\beta - J_\alpha}}{\sqrt{2J_\alpha + 1}} \langle J_\beta || O_k || J_\alpha \rangle_{dST} \qquad (18)$$

Inserting the isospin operator and reducing the dST matrix element in isospin (denoted by the triple bar) gives the following useful result for $e^\mp$ decays

$$\langle J_\beta T_\beta || \tau^\pm O_k || J_\alpha T_\alpha \rangle_{HT} = \mp \frac{(-1)^{J_\beta - J_\alpha}\sqrt{2}}{\sqrt{2J_\alpha + 1}\sqrt{2T_\beta + 1}} C^{T_{3\alpha} \pm 1T_{3\beta}}_{T_\alpha\ 1T_\beta} \langle J_\beta T_\beta ||| \vec{\tau} O_k ||| J_\alpha T_\alpha \rangle$$

$$= \mp\sqrt{\frac{2}{15}} \langle 2^+, 0 ||| \vec{\tau} O_k ||| 2^+, 1 \rangle_{dST} \quad (\Delta T=1 \text{ decays})$$

$$= +\sqrt{\frac{1}{15}} \langle 2^+, 1 ||| \vec{\tau} \vec{O}_k ||| 2^+, 1 \rangle_{dST} \quad (\text{analog decay}) \qquad (19)$$

III. Discussion of the Shell-Model Wave Functions

The wave functions utilized in this work are expansions over the full set of $(0d_{5/2})^{n_1}(1s_{1/2})^{n_2}(0d_{3/2})^{n_3}$ basis vectors, $n_1+n_2+n_3=4$. No excitations from the 0s and 0p orbits (^{16}O core) or into the 0f,1p and higher orbits are allowed. In this space there are 56 components for the A=20, J=2, T=0 wave functions and 66 components for the A=20, J=2, T=1 wave functions. The general conventions for calculations such as have produced the present wave functions are described in reference 6. Specifically, phase conventions are consistent with $\vec{\ell}+\vec{s}$ coupling and with single-particle wave functions which are positive as they approach the origin.

While there exist effective Hamiltonians which yield qualitatively similar results for the quantities calculated here, we have chosen to use the Hamiltonian which yields the best overall reproduction of nuclear observables in the A=18-25 region. This Hamiltonian (consisting of 1- and 2-body terms and with no state or mass dependence) was determined by adjusting the two-body matrix elements of Kuo's interaction so as to obtain a least-squares fit between about 200 experimental binding energies in the A=18-24 region and the eigenvalues of the (presumed) corresponding states.[7] The single-particle energies were chosen to reproduce the experimental spectrum of single-particle states in ^{17}O. This new Hamiltonian can be considered as an improved revision of the Preedom-Wildenthal (PW) interaction.[8] For mass 20 the two interactions yield very similar wave functions.

While the efficacy of the Hamiltonian we have employed here is to an extent established by the excellent reproduction of experimental spectra which it yields,

a more definitive test involves the calculation of other nuclear observables. Principal among the observables against which the present wavefunctions have been tested are single-nucleon spectroscopic factors, magnetic dipole moments, and ft values for Gamow-Teller beta decay. Experimental results for these observables are reproduced very well in general by using unrenormalized single-particle matrix elements and one-body transition densities generated from the wave functions. Experimental values of electric quadrupole observables are also reproduced with these wave functions if the E2 single-particle matrix elements are chosen to reflect added charges to the neutron and proton of about 0.4e.

It is convenient to break calculations of matrix elements of operators into two steps. In the first step, the matrix elements of the bare operators consisting of single-particle annihilation and creation operators coupled to the appropriate angular momentum ΔJ and isospin ΔT are evaluated. These are referred to as the one-body transition densities and are expressed as

$$\mathrm{OBTD}(j_1 j_2 \lambda) = \frac{\langle \psi_f \| (a^\dagger_{j_1} \otimes a_{j_2})_\lambda \| \psi_i \rangle}{\sqrt{2\Delta T+1}\,\sqrt{2\Delta J+1}}, \qquad (20)$$

where ψ_f and ψ_i are the multiparticle wave functions of the states involved in the transition of $\lambda=\Delta J,\Delta T$, and $a^\dagger_{j_1}$ and a_{j_2} are, respectively, a creation operator for a particle in single-particle orbit j_1 and an annihilation operator for a particle in orbit j_2.

These transition densities contain all the usable information about the states in question which originates from the specific shell-model calculations employed. That is, given the active orbits of the model space, any

difference in truncation or Hamiltonian from one calculation to another shows up finally as a different set of transition densities. Putting it another way, the shell model calculation consists of choosing a set of basis vectors and then assigning amplitudes to each basis vector via diagonalization. All of the information obtained from the diagonalization procedure (and contained in the wave functions) which is relevant to a transition operator of rank λ is condensed into the transition density elements. The latter reflect the probability of obtaining the final state wave function by annihilating a particle of orbit j_2 of the initial state and creating a particle in orbit j_1 of the final state. The transition densities between the lowest energy J=2, T=1 and J=2, T=0 wave functions in A=20, for ΔT=1 and ΔJ=1, 2, and 3 are given in Table III.

The remaining step in calculating the value of an observable is to evaluate the matrix elements $\langle \rho_j \| p^{\lambda} \| \rho_j \rangle$ of the operator of interest between the various single-particle states of the model space. These single-particle matrix element values are independent of any particular formulation (i.e., choice of Hamiltonian) of the shell-model calculation. Their values reflect such aspects as the properties of free neutrons and protons, properties of spherical harmonics, and nuclear sizes, etc. Their values may also reflect assumptions about proper renormalizations of the free nucleon properties which may arise from finite basis space effects and/or mesonic effects. The key point is that essentially independent assumptions go into the "shell-model calculation," which results in multi-particle-wave-function amplitudes which in turn lead to the transition densities, and into the evaluation of the single-particle matrix elements of an operator which corresponds to some physical transition process.

We have listed in Table IV the single-particle matrix elements for sd-shell orbits of all the operators under discussion. The radial dependence of the single-particle wave functions is assumed to have a harmonic oscillator form consistent with choice of the size parameter b=1.825. These values can be used not only with other shell-model calculations for A=20 but also for any other sd-shell model calculation in the A=18-38 region.

The combination of the transition densities and the single-particle matrix elements leads to the value of the matrix element of the observable according to the expression

$$\langle \psi_f \| O_p^{\lambda} \| \psi_i \rangle_{dST} = \sum_{j,j'} \langle \rho_j \| p_p^{\lambda} \| \rho_{j'} \rangle \frac{\langle \psi_f \| (a_j^{+} \otimes a_{j'})^{\lambda} \| \psi_i \rangle}{\sqrt{2\Delta T+1}\ \sqrt{2\Delta J+1}} \qquad (21)$$

In Table V we have listed the values obtained for the operators of interest by combining the transition densities of Table III and corresponding values for the second J=2, T=0 and the first J=2, T=1 states of A=20 with the single-particle matrix elements of Table IV. The values of the M_{GT} and M_{M1} operators can be related to results of experimental measurements. The calculated log ft value of 4.87 for the $^{20}F(2^+)$ to $^{20}Ne(2^+, 1.63\ MeV)$ transition is in good agreement with the measured value of 4.97. Measurements of the M1 decay strength between the lowest 2^+, T=1 state in $^{20}Ne(E_x=10.271\ MeV)$ and the 2^+, T=0 first excited state (E_x=1.634 MeV) yield an averaged value of $\Gamma(M1)=4.13\pm0.23$ eV.[9] The theoretical value of 3.4 eV is again in good agreement with this experimental number. If instead of single-particle matrix elements based on the properties of free neutrons and protons, values obtained by slightly adjusting these free-nucleon elements to best fit magnetic moments in the sd-shell are used to calculate this M1 rate, the value changes to 3.7 eV. The E2 partial width for the $(2^+,1)_1 \rightarrow (2^+,0)_1$ decay is calculated to be 3.3×10^{-4} eV, assuming a unit isovector charge. This is considerably smaller than the weak experimental E2 partial width,

which is quoted, without an assigned uncertainty, to be 2×10^{-3} ev.[10] However, the matrix element associated with this decay is reduced from the single-particle value by an order of magnitude. In cases of cancelation this extreme, the final answer is quite sensitive to small details in the wave functions.

The wave functions of the states involved in this transition can be tested beyond aspects which involve their overlap with each other. Both states are populated in single-particle transfer reactions with strengths and mixtures of ℓ-values which are consistent with values calculated from these wave functions. Their electric quadrupole moments and electric quadrupole transition rates in which they participate are reasonable well produced by the present wave functions if protons and neutrons in the model space are assumed to carry 0.4e added charge each. The partial transition width of the decay of the ^{20}Ne(2^+,T=1) state to the (0^+,T=0) ground state is calculated to be 0.046eV ,which compares to the experimental value of 0.028±0.008eV.[9] Finally, the calculated magnetic moments of ^{20}Ne(2^+_1, T=0) and ^{20}F (2^+, g.s.)and^{20}Na(2^+, g.s.) are, respectively, +1.02 n.m., +2.06 n.m. and +0.48 n.m., assuming free-nucleon single-particle matrix elements. The corresponding experimental values are +1.08±08 n.m., +2.09 n.m, and ±0.37 n.m.

We conclude from the preceding paragraphs that matrix elements inferred from directly measured experimental quantities relating to the 2^+, T=1 and 2^+, T=0 states of A=20 are reproduced to within $\sim$ 20% by our shell-model calculations except in the case of highly canceling overlaps. It is on this basis that we hope to get meaningful estimates of the matrix elements of the various operators affecting the details of weak interaction processes.

IV. Discussion of Results

The matrix elements computed for the ^{20}Na(e^+) decays are given in Table V. Except for a common sign change, the ^{20}F matrix elements for the analog decays are identical. Note that for the superallowed ^{20}Na decay to the T=1 level of ^{20}Ne the matrix elements $M_{\sigma L}$ and M_{2y} are zero. This is as expected from charge symmetry arguments.[2]

The form factors derived from the matrix elements are given in Table VI. For comparison with experiment we summarize the b and c form factors for the decay to the 1634 keV level in Table VII. Note that, relative to the theoretical predictions, the experimental value of b is on the high side while that for c is on the low side. As a result, the experimental ratio b/Ac is 25% larger than the theoretical prediction. This ratio is the relevant combination of form factors for the beta-gamma correlation and for the spectrum shape factor and in the following we choose to use the experimental value for the predicted effects. That is, we regard b as given by CVC in terms of the experimental radiative width and c as given by the experimental ft value; the shell model calculations are used merely to determine the remaining form factors.

One more point concerning the ratio b/Ac may be worth noting. According to the expressions in Table I this ratio should be

$$\frac{b}{Ac_1} = (4.7 + \frac{M_L}{M_{GT}}) \frac{g_V}{g_A} \cdot \qquad (22)$$

In many other decays b/Ac is close to 4, which indicates that M_L is smaller than, or comparable to, M_{GT}.[3] However, for the A=20 decays to the 1634 keV level, M_{GT} is somewhat small while M_L, apparently, is not. The above, in fact, implies $M_L/M_{GT} = 5.6$. The result is an enhancement of b relative to

to c and therefore an enhancement of the influence of b on the beta-gamma cancelation and the spectrum shape factors by more than a factor of two compared to normal decays.

We now calculate the beta-gamma correlation parameters for the decays to the 1634 keV levels assuming no second class tensor form factor, $d^{II}=0$. Substituting the experimental values of b and c and the theoretical predictions for the other form factors into equation (7) and expanding to order E^2 gives,

$$B_{\beta\gamma}(e^-) \cong + 0.00128E + 0.00014E^2 \qquad (23)$$

$$B_{\beta\gamma}(e^+) \cong - 0.00310E + 0.00016E^2 \ . \qquad (24)$$

Here E is the total energy in MeV. The correlation parameters calculated with the complete expression of equation (7) (which differ slightly from equations (23) and (24)) are plotted in Figure 2 as a function of the kinetic energy. It should be noted that a significant quadratic effect is expected, particularly for the ^{20}Na decay. Along with the complete correlation we also illustrate the contributions of selected form factors: (1) weak magnetism only and (2) weak magnetism and first class tensor, d^I. Note that the influence of the first class d^I term is significant; at 5MeV B is lowered by 0.6% due to d^I. When the higher order terms are included B is raised again but not enough to compensate for the d^I term.

Note that because of the difference in end-point energies the contribution of the higher order terms g and j_2 are not symmetric for both decays. the g-term can be obtained by CVC from the radiative width Γ_{E2}, when an experimental value for this is available, but there is no way to determine j_2 except from a calculation. The j_2 term does contribute to the quadratic energy dependence of the correlation parameter but the main quadratic effect is due to j_3. A measurement of the quadratic effect therefore does not help to fix j_2 except perhaps by confirming the calculation of j_3, and indirectly

that of j_2. As an indication that the uncertainty in j_2 is not a serious problem note that the difference of the correlation parameters, $B(e^-) - B(e^+)$, at 5 MeV is expected to be 2.5% due to b. The contribution to this difference due to j_2 is only 0.08% and therefore it is probably safe to trust the calculation. However, if the calculation of j_2 is too small by a factor of 10, then its contribution to the difference of the correlation parameters is 1/3 that of the weak magnetism term and this could be misinterpreted as a contribution from d^{II}. Thus caution must be exercised in setting a limit on d^{II} from the correlation parameters.

Next we compute the spectral shape factor $h_1(E)$ for the same transitions to the 1634 keV level. Again, using the experimental values for b and c and the computed values for the other form factors and normalizing to $h_1(E = mc^2)$ we obtain

$$S(E)_{e^-} = \frac{h_1^-(E)}{h_1^-(mc^2)} = 1 + 0.0117E - 0.000347E^2 - 0.00200/E \qquad (25)$$

$$S(E)_{e^+} = \frac{h_1^+(E)}{h_1^+(mc^2)} = 1 - 0.00506E - 0.000320E^2 + 0.00102/E. \qquad (26)$$

The results are plotted in figure 3. It may be noted that the deviation from the allowed shape (S = 1) is very sizeable. The deviation is mainly a linear effect due to the weak magnetism form factor but there is also a noticeable quadratic curvature which comes about from the q^2 dependence of the Gamow-Teller form factor (c_2)

Finally we compute the βα correlation corresponding to the ^{20}Na decay to the 7421 keV level of ^{20}Ne. Using equation (10) and the computed form

factors of Table VI we obtain

$$B_{\beta\alpha}(e^+) = -0.00286E - 0.00006E^2 \qquad (27)$$

This correlation has been measured by Oakey and Macfarlane[11] with the result $B(\bar{E} = 3.3\ \text{MeV}) = -0.083 \pm 0.013$. According to equation (27) we would expect $B = -0.010$ which is in poor agreement with this experimental result. The higher order E^2 term has very little effect in this case, contrary to the speculation of Oakey and Macfarlane. For the kinematic correlation parameter, Oakey and Macfarlane obtain $A_{exp} = -0.026 \pm 0.001$ while the prediction given by equation (9) is $A = -0.0086$. Thus, the agreement between experiment and theory is poor for both correlation parameters. A recent measurement of the B correlation parameter made by Freedman and Gagliardi[12] yields a value much smaller than the Oakey-Macfarlane value and in reasonable agreement with the prediction. Thus the discrepancy is very likely associated with experimental difficulties.

We have not attempted here to make further detailed comparisons of the present calculations with the fresh data being accumulated[15,17-19] on the A=20 decays by several groups, since the majority of these are not yet in the open literature.

References

1. S. Weinberg, Phys. Rev. 112, 1375 (1958).
2. B. R. Holstein, Rev. Mod. Phys. 46, 789 (1974).
3. F. P. Calaprice and B. R. Holstein, to be published in Nuclear Physics. See also H. Behrens and J. Jänecke, Numerical Tables for Beta Decay and Electron Capture, Landolt-Börnstein, New Series, Vol. I/4, Berlin-Heidelberg - New York, Springer (1969).
4. B. R. Holstein, W. Shanahan and S. B. Treiman, Phys. Rev. C5, 1849 (1972).
5. A. de-Shalit and I. Talmi, Nuclear Shell Theory. New York and London, Academic Press (1963).
6. E. C. Halbert, J. B. McGrory, B. H. Wildenthal, S. P. Pandya, Adv. Nuclear Phys. Vol 4, Plenum Press, N. Y. (1971).
7. W. Chung and B. H. Wildenthal, to be published.
8. B. M. Preedom and B. H. Wildenthal, Phys. Rev. C6, 1633 (1972).
9. K. Fifield, F. P. Calaprice, K. Allen, to be published; (see also P.D. Ingalls, Nucl. Phys. A265, 93 (1976).
10. J. D. Pearson and R. H. Spear, Nuc. Phys. 54, 434 (1964).
11. N. S. Oakey and R. D. Macfarlane, Phys. Rev. Letters 25, 170 (1970).
12. S. J. Freedman and C. Gagliardi, Princeton University, Private Communication (1976).
13. D. F. Torgenson, K. Wien, Y. Fares, N. S. Oakey, R. D. Macfarlane and W. A. Ianford, Phys. Rev. C8, 161 (1973).
14. A. Gallman, F. Jundt, E. Adanides and D. E. Alburger, Phys. Rev. 179, 921 (1969).
15. F.P. Calaprice and D.E. Alburger, to be published; (see also Ref. 17).
16. F. Boehm, V. Soergel and B. Stech, Phys. Rev. Letts. 1, 77 (1958).
17. H. Genz, A. Richter, B.M. Schmitz, and H. Behrens, Nucl. Phys. A267, 13 (1976).
18. R.H. Tribble, private communication.
19. N. Rolin, J.P. Deutsch, D. Favart, M. Lebrun, and R. Prieels, private communication.

Figure Captions

Figure 1. Simplified decay schemes of the T=1 states of the A=20 system. The decays to the 1634 keV level of ^{20}Ne are considered in the text as candidates for a test of the CVC theory and for a search for second class currents. Radiative widths are taken from ref. 9, ^{20}Na ft values from ref. 13 and ^{20}F ft value from ref. 14. The limit for the ^{20}F ground state transition is taken from a new unpublished measurement[15].

Figure 2. Theoretical beta gamma correlation coefficients for the ^{20}F - ^{20}Na mirror decays to the 1634 keV level of ^{20}Ne. The solid line is computed assuming no second class terms and with all first class form factors to order E^2/M^2. The correlation parameters calculated with only the weak magnetism (b) and first class tensor (d) form factors are also shown. The experimental point is that of Boehm et. al (ref. 16).

Figure 3. Theoretical spectrum shape factors for the ^{20}F - ^{20}Na decays to the 1634 keV level of ^{20}Ne. The large linear effect is due to the weak magnetism form factor, as determined by CVC from the M1 radiative width of the analog decay of ^{20}Ne. A small quadratic effect is expected from the q^2 dependence of the Gamow-Teller form factor.

Table I. The Nuclear Form Factors

$$c_1 \simeq g_A M_{GT}$$

$$c_2 \simeq \frac{1}{6} g_A \left[M_{\sigma r^2} + \frac{1}{\sqrt{10}} M_{1y} \right]$$

$$b \simeq A \left[g_M M_{GT} + g_v M_L \right]$$

$$d^I = A g_A M_{\sigma L}$$

$$f = \sqrt{\frac{2}{3}}\, M\Delta\, g_v\, M_Q/(\hbar c)^2$$

$$g = -\frac{4}{3} M^2\, g_v\, M_Q/(\hbar c)^2$$

$$j_k = -\frac{2}{3} M^2\, g_A\, M_{ky}/(\hbar c)^2$$

$$h = \frac{-2}{\sqrt{10}} M^2 g_A\, M_{1y}/(\hbar c)^2 - A^2 g_P M_{GT}$$

$g_A \simeq 1.23$

$g_M = 4.70$, $g_v = 1.00$

A = mass number

$M = \frac{1}{2}(M_i + M_f)$ = nuclear mass

$\Delta = M_i - M_f$ = nuclear energy release

$g_P \approx -\left(\frac{2m_p}{m_\pi}\right)^2 g_A = -222$

Table II. The Nuclear Matrix Elements

Matrix Element	Operator Form
M_{GT}	$\langle \beta \| \sum \tau_i^{\pm} \vec{\sigma}_i \| \alpha \rangle$
$M_{\sigma r^2}$	$\langle \beta \| \sum \tau_i^{\pm} \vec{\sigma}_i r_i^2 \| \alpha \rangle$
M_L	$\langle \beta \| \sum \tau_i^{\pm} \vec{r}_i \| \alpha \rangle$
$M_{\sigma L}$	$\langle \beta \| \sum \tau_i^{\pm} i\vec{\sigma}_i \times \vec{r}_i \| \alpha \rangle$
M_Q	$\sqrt{\frac{4\pi}{5}} \langle \beta \| \sum \tau_i^{\pm} r_i^2 Y_2(\hat{r}_i) \| \alpha \rangle$
M_{ky}	$\sqrt{\frac{16\pi}{5}} \langle \beta \| \sum \tau_i^{\pm} \sigma_i^2 C_{12k}^{nn'k} \sigma_{in} Y_2^{n'}(\hat{r}_i) \| \alpha \rangle$

$$\langle \psi_f \| (a^\dagger_{j_1} \times a_{j_2})_\lambda \| \psi_i \rangle (2\Delta T+1)^{-1/2} (2\Delta J+1)^{-1/2}$$

j_1 j_2	$\Delta J=1, \Delta T=1$	$\Delta J=2, \Delta T=1$	$\Delta J=3, \Delta T=1$
$\frac{5}{2}$ $\frac{5}{2}$	+0.2763	-0.3176	-0.2446
$\frac{5}{2}$ $\frac{1}{2}$	0	-0.0250	+0.0034
$\frac{5}{2}$ $\frac{3}{2}$	-0.0765	+0.0120	+0.1495
$\frac{1}{2}$ $\frac{5}{2}$	0	+0.2985	-0.3565
$\frac{1}{2}$ $\frac{1}{2}$	+0.0202	0	0.0
$\frac{1}{2}$ $\frac{3}{2}$	+0.1087	-0.0989	0.0
$\frac{3}{2}$ $\frac{5}{2}$	-0.1646	-0.1480	+0.0427
$\frac{3}{2}$ $\frac{1}{2}$	-0.0156	+0.0116	0.0
$\frac{3}{2}$ $\frac{3}{2}$	+0.0310	+0.0651	+0.0315

Table III One-body transition densities between the first shell-model A=20, J=2, T=1 (ψ_i) and A=20, J=2, T=0, (ψ_f) wave functions.

Table IV Single-particle matrix elements of relevant operators for the $0d_{5/2}$, $1s_{1/2}$, and $0d_{3/2}$ single-particle wave functions. Harmonic oscillator radial dependence with b=1.825F has been assumed and the radial integrals are

$$\langle 0d|r^2|0d\rangle = \langle 1s|r^2|1s\rangle = \frac{7}{2}\nu^{-1} = \frac{7}{2}b^2 = 11.66F^2$$

$$\langle 0d|r^2|1s\rangle = \langle 1s|r^2|0d\rangle = -\sqrt{10}\nu^{-1} = -\sqrt{10}b^2 = -10.53F^2.$$

Entries with asterisk (*) denote that $\langle \rho j|0|\rho j'\rangle$ has opposite sign relative to $\langle \rho j'|0|\rho j\rangle$; for those with no *, the two are equal.

$$\langle \rho j \| O_p(\Delta T=1) \| \rho j' \rangle_{dST}$$

Op	$\frac{5}{2}$, $\frac{5}{2}$	$\frac{5}{2}$, $\frac{1}{2}$	$\frac{5}{2}$, $\frac{3}{2}$	$\frac{1}{2}$, $\frac{1}{2}$	$\frac{1}{2}$, $\frac{3}{2}$	$\frac{3}{2}$, $\frac{3}{2}$
M_{GT}	3.549	0	-3.794*	+2.999	0	-1.897
M_Q	-16.72	-14.13	-8.360*	0	-11.54*	-12.77
$M_{\sigma r^2}(F^2)$	+41.38	0	-44.24*	+34.98	0	-22.12
M_L	7.099		1.897*			5.692
$M_{\sigma L}$	0	0	-9.486	0	0	0
M_{ky} K=1	+14.95	0	+13.99*	0	+28.26*	-27.98
K=2	0	+23.08*	+34.13	0	+28.26	0
K=3	-44.86	-43.17	+24.42*	0	0	+7.477

Table V. Values of the $^{20}Na \rightarrow {}^{20}Ne$ total multi-particle matrix elements for three final states of ^{20}Ne as obtained from one-body transition densities such as those of Table III and the single-particle matrix elements of Table IV.

J_f, T_f	M_{GT}	$M_{\sigma r}{}^2$	M_L	$M_{\sigma L}$	M_Q	M_{1y}	M_{2y}	M_{3y}
$2_1^+,0$	+0.237	$+2.76F^2$	+0.842	+0.835	$+0.203F^2$	$+2.92\ F^2$	$-5.32\ F^2$	$+10.6\ F^2$
$2_2^+,0$	-0.495	$-5.77F^2$	-0.416	-0.902	$+0.163F^2$	$-0.084F^2$	$-1.99\ F^2$	$-4.01\ F^2$
$2_1^+,1$	-0.344	$-4.01F^2$	+0.248	0.0	$+2.04\ F^2$	$+2.10F^2$	$0.0\ F^2$	$-1.66\ F^2$

Table VI. Form factors for ^{20}Na transitions to three states of ^{20}Ne

Form factor	$T=0, J=2_1$	$T=0, J=2_2$	$T=1, J=2_1$
$c_1 = g_A M_{GT}$	+0.292	-0.609	-0.423
$c_2 = \frac{1}{6} g_A \left(M_{\sigma r}{}^2 + \frac{1}{\sqrt{10}} M_{1y} \right)$	$+0.755\ F^2$	$-1.19\ F^2$	$-0.686F^2$
$b = A \left(g_M M_{GT} + g_v M_L \right)$	+39.1	-54.9	-27.4
$d^I = g_A A M_{\sigma L}$	+20.5	-22.2	0.0
$f = \sqrt{\frac{2}{3}} M \Delta g_v M_Q / (\hbar c)^2$	$-.469\ {}^{20}F$ $+.932\ {}^{20}Na$	+ 0.380	+ 2.48
$g = \frac{-4}{3} M^2 g_v M_Q / (\hbar c)^2$	-2.41×10^3	-1.94×10^3	-2.42×10^4
$j_2 = \frac{-2}{3} M^2 g_A M_{2y} / (\hbar c)^2$	$+3.89 \times 10^4$	$+1.45 \times 10^4$	0.0
$j_3 = \frac{-2}{3} M^2 g_A M_{3y} / (\hbar c)^2$	-7.75×10^4	$+2.93 \times 10^4$	1.22×10^4
$h = \frac{-2}{\sqrt{10}} M^2 g_A M_{1y} / (\hbar c)^2 - A^2 g_P M_{GT}$	$+7.43 \times 10^2$	-4.34×10^4	-4.51×10^4

Table VII. Comparison of Form Factors for the Transition to the 1634 keV Level

	b	c	b/Ac
Experiment*	42.7 ± 1.2	0.256 ± 0.006	8.34 ± 0.30
Theory	39.1	0.292	6.70

*The signs are not obtained from the experimental decay rates. They are assumed to be the same as the theoretical predictions.

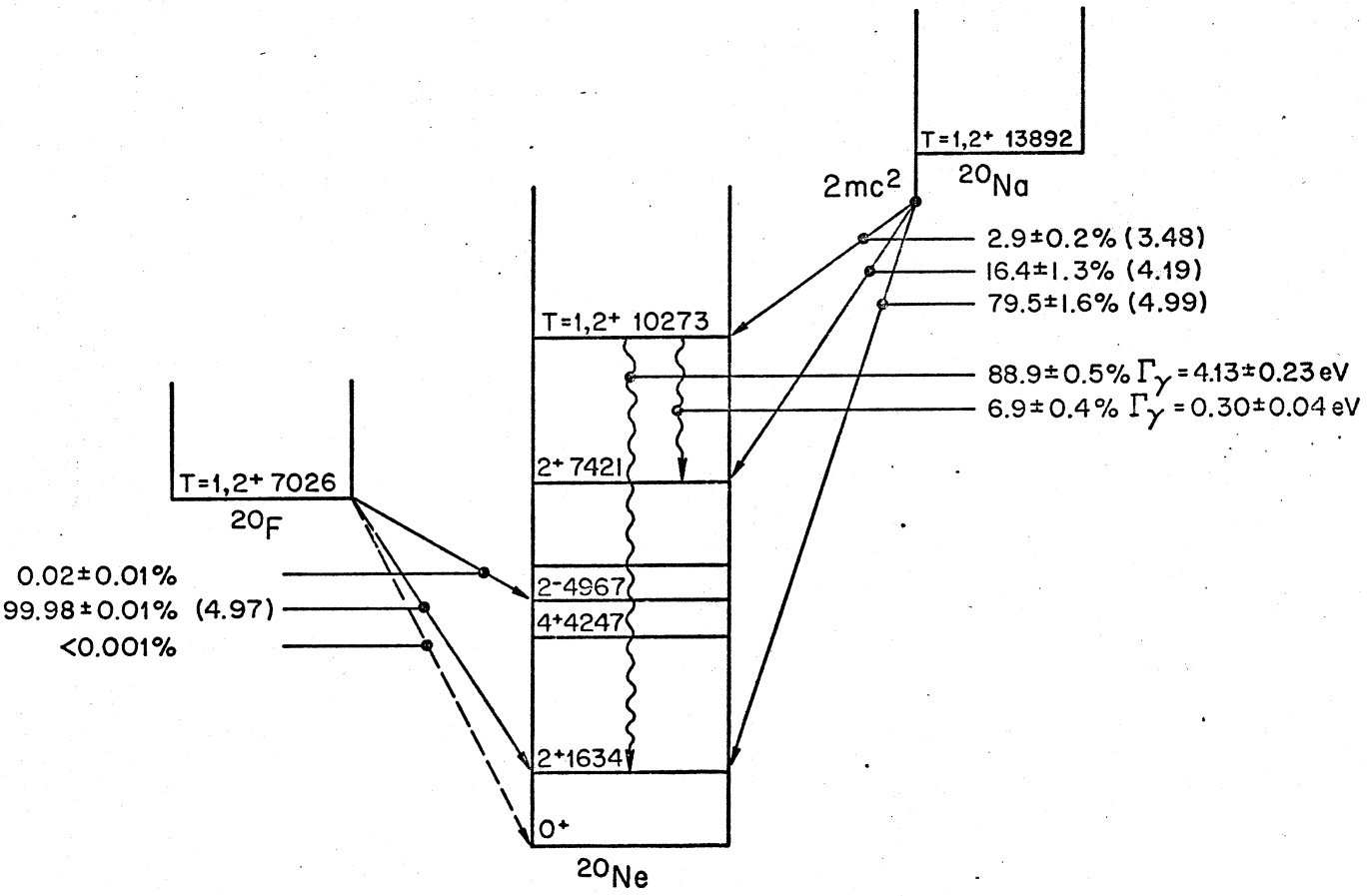

Fig. 1

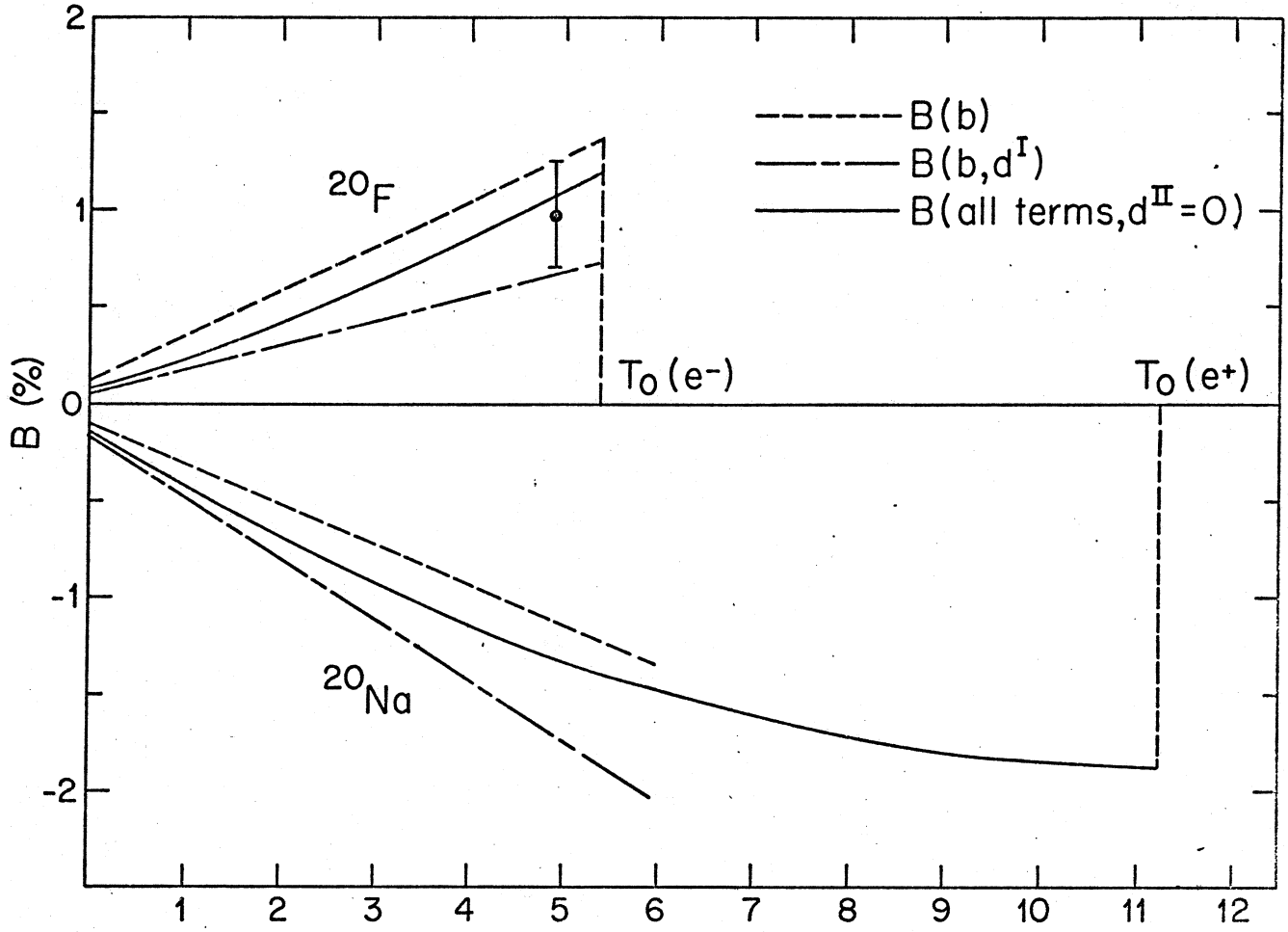
B(b)
B(b,d^I)
B(all terms,d^II=0)
20F
20Na
T0(e-)
T0(e+)
B (%)
KINETIC ENERGY (MeV)

Fig. 2

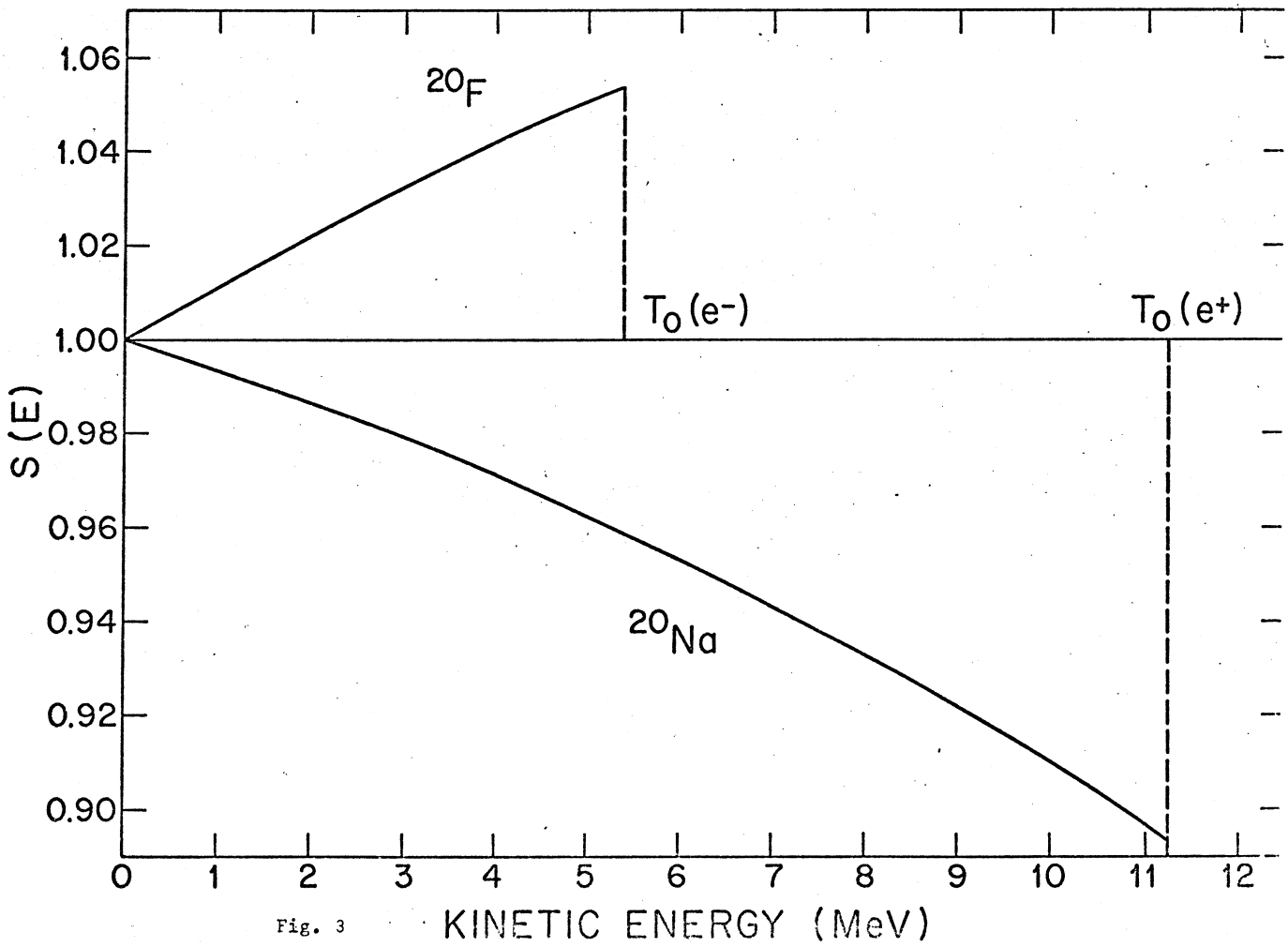
20F
20Na
T0(e-)
T0(e+)
S(E)
KINETIC ENERGY (MeV)

Fig. 3